

Org. Chem. Res., Vol. 7, No. 2, 206-215, July 2021.

DOI: 10.22036/org.chem.2023.378731.1283

Magnetic Nanoparticles Coated with Ethylenediamine Sulfone as an Efficient Heterogeneous Catalyst for the Green Synthesis of 2-Arylbenzoxazoles

F. Hakimi, E. Golrasan and H. Shademanpoor

Department of chemistry, Faculty of science, Payame Noor University, Tehran, Iran

(Received 29 December 2022, Accepted 1 September 2023)

In this investigation, an efficient nanomagnetic heterogeneous catalyst of $\text{Fe}_3\text{O}_4@\text{SiO}_2@(\text{CH}_2)_3\text{-en-SO}_3\text{H}/\text{H}_2\text{SO}_4$ was prepared. Then it was used for the synthesis of 2-arylbenzoxazoles by the cyclocondensation reaction of aromatic aldehydes with 2-aminophenol under solvent-free conditions. The catalyst of $\text{Fe}_3\text{O}_4@\text{SiO}_2@(\text{CH}_2)_3\text{-en-SO}_3\text{H}/\text{H}_2\text{SO}_4$, was synthesized by the immobilization of sulfonated ethylenediamine on the silica-supported magnetic nanoparticles. The catalyst can be recycled magnetically and can be reused several times without a significant decrease in the activity of the catalyst. The present method has several advantages such as excellent efficiency, convenient purification, mild reaction conditions, easy operation and short reaction time. Also, the nanomagnetic heterogeneous catalyst is found to be an economical and reusable catalyst with low catalytic loading, a suitable catalyst, stable in air and humidity, heterogeneous and green catalytic.

Keywords: Heterogeneous catalyst, Nanomagnetic $\text{Fe}_3\text{O}_4@\text{SiO}_2@(\text{CH}_2)_3\text{-en-SO}_3\text{H}/\text{H}_2\text{SO}_4$, Solvent free, Benzoxazole derivatives

INTRODUCTION

Benzoxazole and its derivatives have attracted considerable attention due to their presence in the structure of numerous natural products and biologically active molecules. The compounds possessing benzoxazole scaffold exhibit a wide range of biological and pharmaceutical activities such as anticancer, antimicrobial, anti-HIV, antifungal, antiviral and antibacterial activities [1-3]. There are several synthetic procedures for the synthesis of benzoxazole derivatives, two of the most common of which are the reaction of 2-aminophenol with carboxylic acid derivatives [4-5] and cyclocondensation of 2-aminophenol with aldehydes in the presence of various catalysts [6-16]. Most of these methods have practical limitations such as the use of toxic materials and hazardous organic solvents, the use of large amounts of catalysts, harsh reaction conditions and long reaction times. Therefore, there is still a need to develop

green, efficient, simple and mild methods for the synthesis of 2-arylbenzoxazoles.

Homogeneous catalysts usually have high selectivity and activity due to their solubility in the reaction environment, the low chemical and thermal stability of these catalysts has limited their performance, and their recovery from the reaction mixture is mostly difficult. Reducing these limitations is still a challenge for chemical scientists [17-19]. Heterogenization of soluble catalysts is one of the simplest solutions for this problem. The immobilization of homogeneous catalysts on insoluble materials has many advantages, including easy recovery of the catalyst, high stability, and resistance to degradation [20-21].

The functionalization of magnetic nanoparticles and the stabilization of homogeneous catalysts on the surface of MNPs have been widely studied in academic and industrial centers due to their wide applications in materials science, chemistry, medicine and catalysis [22-25].

Functionalization of magnetic nanoparticles and immobilization of homogeneous catalysts on the surface of

*Corresponding author. E-mail: fatemeh.hakimi@yahoo.com

MNPs have been widely studied in industries and academic centers due to their potential wide applications as catalysis in materials science, medicine and chemistry [26-29]. MNPs can be used as solid support materials for the heterogenization of catalysts due to their high surface area, easy processing, diversity and availability. These types of nanocatalysts are very important in green chemistry due to their high activity, stability, environmental friendliness and reusability [30-32]. Green chemistry has attracted the attention of chemists and researchers in recent years [29]. By designing reactions that minimize the use and production of hazardous chemicals and also avoid the use of organic solvents, using safer alternative solvents or performing reactions in solvent-free conditions can solve the toxicity and disposal problems of traditional organic solvents. And focuses on technological approaches to prevent pollution [30-32].

Considering the catalytic importance of functionalized magnetic nanoparticles and the articles recently reported for the synthesis of heterocyclic compounds [33-36], now the synthesis of a new nanomagnetic solid acid catalyst ($\text{Fe}_3\text{O}_4@\text{SiO}_2@(\text{CH}_2)_3\text{-en-SO}_3\text{H}/\text{H}_2\text{SO}_4$) and we report its characterization with different techniques and the catalytic performance of the supported organic catalyst for the preparation of 2-arylbenzoxazoles through the reaction of aryl aldehydes with 2-aminophenol (Scheme 1) was investigated.

EXPERIMENTAL

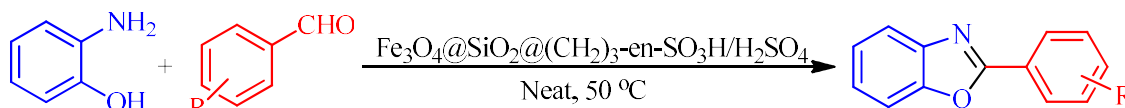
General

All materials used were purchased from Merck and Sigma-Aldrich. Magnetite nanoparticles and Fe_3O_4 nanoparticles coated with silica were prepared according to

previously reported methods [37]. Thin layer chromatography on silica gel plates SILG/UV 254 was used to investigate the progress of the reactions. The melting point of products was measured by electro-thermal device 9200 in open capillary tubes. The functional groups of the synthesized compounds were confirmed using the infrared spectrum on KBr disks and Shimadzu IRPrestige-21 spectrophotometer. The crystalline structure of the nanoparticles was identified by XRD analysis using a PANalytical X'Pert Pro X-ray diffract meter. FESEM images and EDS spectra of catalyst nanoparticles were obtained with a Zeiss-Sigma VP microscope. TEM images of the catalyst were observed with a Zeiss Em10C electron microscope. TGA was recorded on a TA-Q600 instrument in an air atmosphere in the temperature range of 25-800 °C at a rate of 10 °C/min. The VSM was measured at room temperature at the Desert Magnet Co., Kashan and Iran.

Synthesis of Magnetic Nanoparticles-supported Sulfonated Ethylenediamine

Initially, $\text{Fe}_3\text{O}_4@\text{SiO}_2$ (2 g) was dispersed in toluene (100 ml) and ultrasonicated for 20 min. Then, 2 ml of (3-chloropropyl) triethoxysilane was added to it and stirred for 12 h under reflux conditions. $\text{Fe}_3\text{O}_4@\text{SiO}_2@(\text{CH}_2)_3\text{-Cl}$ nanoparticles were magnetically separated, washed with EtOH and dried at 60 °C. In the second step, 10 ml of ethylenediamine was added to a mixture of 2 g of $\text{Fe}_3\text{O}_4@\text{SiO}_2@(\text{CH}_2)_3\text{-Cl}$ in acetonitrile (200 ml) and stirred under reflux for 12 h. Then, $\text{Fe}_3\text{O}_4@\text{SiO}_2@(\text{CH}_2)_3\text{-en}$ nanoparticles were collected with magnetite, washed with ethanol and dried at 60 °C. In the third step, to a mixture of ethylenediamine immobilized on MNPs (2 g) in CH_2Cl_2 (50 ml), 2 ml of chlorosulfonic acid was added dropwise and stirred at room temperature for 6 h until $\text{Fe}_3\text{O}_4@\text{SiO}_2@$



Scheme 1. Synthesis of 2-arylbenzoxazoles in the presence of $\text{Fe}_3\text{O}_4@\text{SiO}_2@(\text{CH}_2)_3\text{-en-SO}_3\text{H}/\text{H}_2\text{SO}_4$

(CH₂)₃-en-SO₃H/Cl can be produced. Was separated, washed with EtOH and dried at 60 °C. Finally, to a mixture of produced MNPs (1.5 g) in water (20 ml), potassium hydrogen sulfate (excess, ~0.5 g) was added and stirred overnight at room temperature. The product was magnetically separated, washed with EtOH and dried under vacuum at room temperature.

General Method for the Synthesis of 2-Arylbenzoxazoles Using Fe₃O₄@SiO₂@(CH₂)₃-en-SO₃H/H₂SO₄

To the mixture of 2-aminophenol (1 mmol) and aromatic aldehydes (1 mmol) catalyst (0.03 g, 7 mol%) was added, and the reaction mixture was stirred at 50 °C and solvent-free conditions for a suitable time (Table 2). After completion of the reaction, as indicated by TLC (1:3 n-hexane/ethanol), hot ethanol (3 ml) was added to the mixture and stirred for 5 min. The nanocatalysts were removed with an external magnet and the desired product was isolated and purified with hot EtOH. By comparing their physical and spectroscopic data, they were identified with authentic samples.

Selected Characterization Data

2-Phenylbenzoxazole (Table 3, Entry 1). FT-IR (KBr): ν (cm⁻¹) = 1241, 1282, 1450, 1483, 1532, 1626, 2855, 2924, 3058; ¹H NMR (CDCl₃, 400 MHz): δ (ppm) = 7.30-7.36 (m,

2H), 7.48-7.52 (m, 3H), 7.53-7.61 (m, 1H), 7.75-7.82 (m, 1H), 8.24-8.28 (m, 2H); ¹³C NMR (CDCl₃, 100 MHz): δ (ppm) = 111.8, 118.2, 122.9, 123.8, 128.3, 129.3, 130.6, 141.6, 150.9, 163.8.

2-(2-Chlorophenyl) benzoxazole (Table 3, Entry 4).

FT-IR (KBr): ν (cm⁻¹) = 1226, 1279, 1458, 1481, 1576, 1617, 2868, 2930, 3047; ¹H NMR (CDCl₃, 400 MHz): δ (ppm) = 7.34-7.47 (m, 4H), 7.56-7.66 (m, 2H), 7.86-7.92 (m, 1H), 8.16 (dd, *J* = 1.8, 7.3 Hz, 1H); ¹³C NMR (CDCl₃, 100 MHz): δ (ppm) = 110.8, 119.2, 123.7, 124.4, 126.8, 128.6, 129.1, 131.4, 133.6, 136.5, 141.6, 150.1, 161.1.

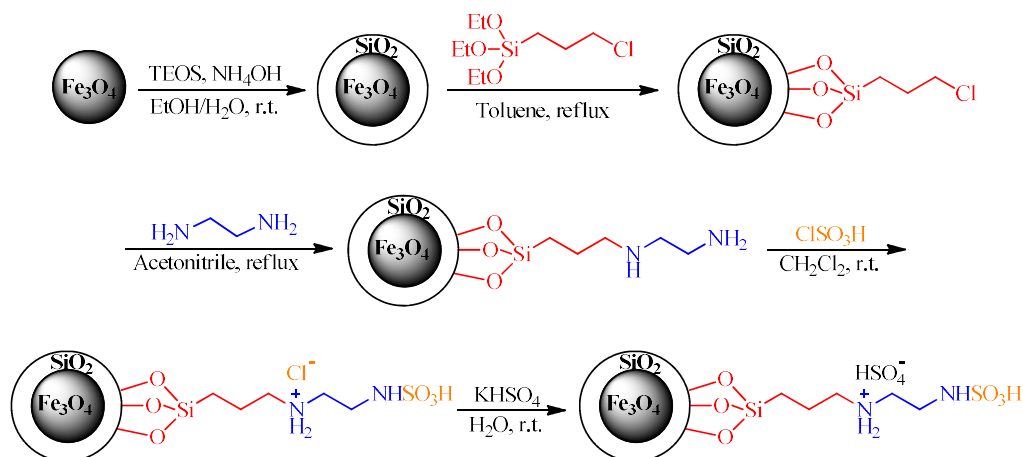
2-(Furan-2-yl) benzoxazole (Table 3, Entry 12).

FT-IR (KBr): ν (cm⁻¹) = 1270, 1462, 1486, 1553, 1607, 2895, 2956, 3052; ¹H NMR (CDCl₃, 400 MHz): δ (ppm) = 6.61-6.65 (m, 1H), 7.26-7.32 (m, 1H), 7.42-7.48 (m, 2H), 7.56-7.61 (m, 1H), 7.72 (d, *J* = 7.8 Hz, 1H), 7.76-7.84 (m, 1H); ¹³C NMR (CDCl₃, 100 MHz): δ (ppm) = 110.5, 112.6, 115.6, 120.2, 124.6, 125.7, 141.4, 142.1, 146.1, 150.3, 155.1.

RESULTS AND DISCUSSION

Catalyst Characterization

Magnetic nanocatalysts of Fe₃O₄@SiO₂@(CH₂)₃-en-SO₃H/H₂SO₄ were prepared by the method shown in Scheme 2. Silica-coated magnetite nanoparticles were prepared according to the reported method [37].



Scheme 2. The synthetic pathway for Fe₃O₄@SiO₂@(CH₂)₃-en-SO₃H/H₂SO₄ nanocatalysts

Then (3-chloropropyl) triethoxysilane was added and refluxed in toluene. Ethylene diamine caused stabilization on the surface of magnetic nanoparticles by nucleophilic attack on $\text{Fe}_3\text{O}_4@\text{SiO}_2@(\text{CH}_2)_3\text{-Cl}$. MNPs were sulfonated by adding chlorosulfonic acid and then treated with potassium hydrogen sulfate aqueous solution at room temperature.

FT-IR spectra of Fe_3O_4 , $\text{Fe}_3\text{O}_4@\text{SiO}_2$, $\text{Fe}_3\text{O}_4@\text{SiO}_2@(\text{CH}_2)_3\text{-Cl}$, $\text{Fe}_3\text{O}_4@\text{SiO}_2@(\text{CH}_2)_3\text{-en}$, $\text{Fe}_3\text{O}_4@\text{SiO}_2@(\text{CH}_2)_3\text{-en-SO}_3\text{H/HCl}$ and $\text{Fe}_3\text{O}_4@\text{SiO}_2@(\text{CH}_2)_3\text{-en-SO}_3\text{H/H}_2\text{SO}_4$ is presented in Fig. 1 as a stacked spectrum. In the vibrational spectrum of the catalyst ($\text{Fe}_3\text{O}_4@\text{SiO}_2@(\text{CH}_2)_3\text{-en-SO}_3\text{H/H}_2\text{SO}_4$), a strong peak at 559 cm^{-1} is assigned to Fe-O stretching vibration and three important peaks are assigned to Si. -O-Si asymmetric stretching, symmetric stretching and bending vibrations are observed at 1080 , 964 and 463 cm^{-1} respectively [37]. The introduction of ethylenediamine is confirmed by the N-H bending absorption bands at 1512 cm^{-1} [38]. The symmetric and asymmetric O=S=O stretching absorption bands at about 1050 to 1200 cm^{-1} overlap with the Si-O-Si asymmetric stretching vibrations [39]. The existence of bandwidth at 3414 cm^{-1} related to O-H stretching absorption and O-H deformation vibration near 1628 cm^{-1} confirmed the presence of SO_3H moieties in the catalyst structure [40].

The FESEM image of $\text{Fe}_3\text{O}_4@\text{SiO}_2@(\text{CH}_2)_3\text{-en-SO}_3\text{H/H}_2\text{SO}_4$ in Fig. 2 shows that the prepared nanocatalysts have an almost spherical morphology. And the SEM image shows that the size of the catalyst particles is less than 100 nm . Also, the TEM image confirmed the core-shell structure of the nanocatalysts and confirms the results obtained from SEM (Fig. 3). The black dots in the TEM image represent the core of the Fe_3O_4 nanoparticles, indicating that the MNPs are successfully surrounded by a silica shell.

From the SEM analysis of the catalyst, the EDS result obtained in Fig. 4 shows the presence of sulfur, nitrogen, oxygen, carbon, silicon and iron in the structure of the catalyst as expected. The peak of gold in EDX analysis is observed due to the gold coating that was deposited on the

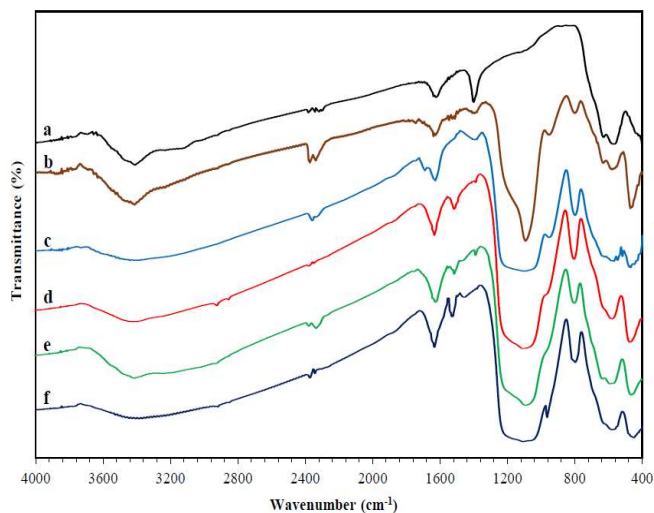


Fig. 1. A stacked infrared spectrum of (a) Fe_3O_4 , (b) $\text{Fe}_3\text{O}_4@\text{SiO}_2$, (c) $\text{Fe}_3\text{O}_4@\text{SiO}_2@(\text{CH}_2)_3\text{-Cl}$, (d) $\text{Fe}_3\text{O}_4@\text{SiO}_2@(\text{CH}_2)_3\text{-en}$, (e) $\text{Fe}_3\text{O}_4@\text{SiO}_2@(\text{CH}_2)_3\text{-en-SO}_3\text{H/HCl}$ and (f) $\text{Fe}_3\text{O}_4@\text{SiO}_2@(\text{CH}_2)_3\text{-en-SO}_3\text{H/H}_2\text{SO}_4$.

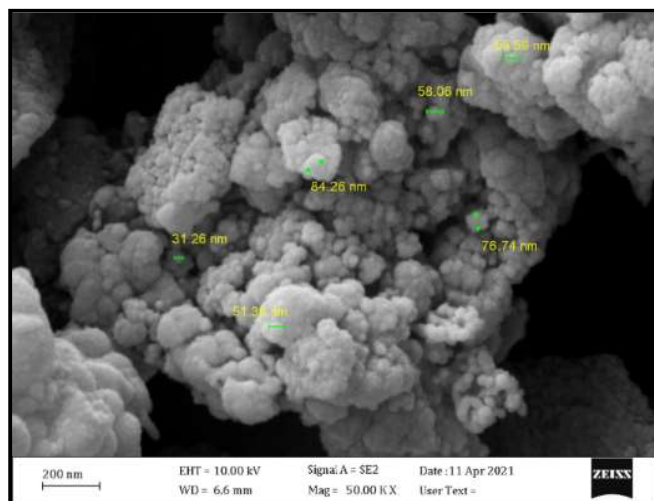


Fig. 2. FESEM image of $\text{Fe}_3\text{O}_4@\text{SiO}_2@(\text{CH}_2)_3\text{-en-SO}_3\text{H/H}_2\text{SO}_4$.

samples before FESEM/EDX analysis.

The room temperature magnetic properties of bare Fe_3O_4 , $\text{Fe}_3\text{O}_4@\text{SiO}_2$ core-shell nanostructure and $\text{Fe}_3\text{O}_4@\text{SiO}_2@(\text{CH}_2)_3\text{-en-SO}_3\text{H/H}_2\text{SO}_4$ nanocatalysts were investigated

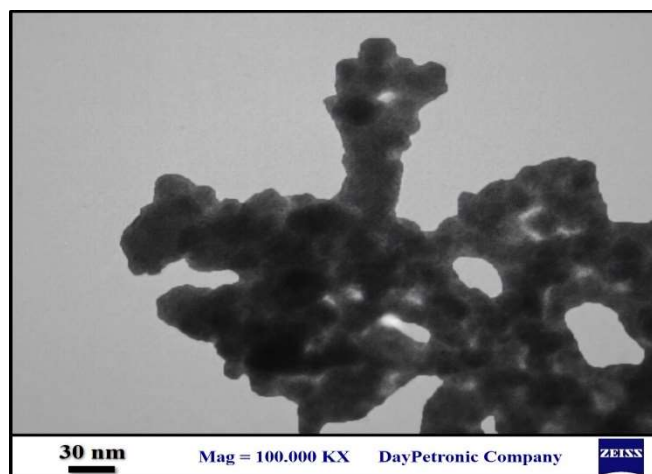


Fig. 3. TEM image of $\text{Fe}_3\text{O}_4@SiO_2@(CH_2)_3\text{-en-SO}_3\text{H}/H_2\text{SO}_4$.

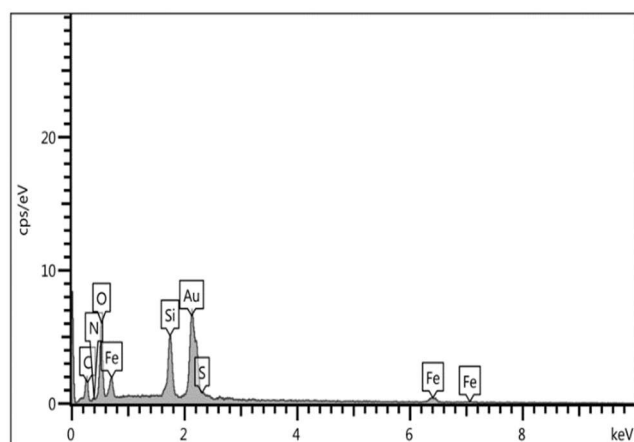


Fig. 4. EDS spectrum of $\text{Fe}_3\text{O}_4@SiO_2@(CH_2)_3\text{-en-SO}_3\text{H}/H_2\text{SO}_4$.

using a vibrating sample magnetometer (VSM) (Fig. 5). The magnetization curves show that the saturation magnetization of the catalyst is 24 emu/g, which is much lower than that of bare magnetic iron oxide (58 emu/g) and $\text{Fe}_3\text{O}_4@SiO_2$ (42 emu/g). Due to the presence of non-magnetic materials such as silica shell, binder and ethylene diamine sulfone, it reduces the magnetic saturation of the catalyst at the level of nanoparticles.

XRD analysis in the 2θ region 10-80 degree crystallinity of magnetite nanoparticles in the synthesized catalyst was obtained (Fig. 6). As seen in the XRD pattern, the intensity and position of the diffraction peaks at $2\theta = 30.40^\circ$, 35.72° , 43.30° , 53.97° , 57.35° and 63.04° are completely consistent with the Fe_3O_4 pattern ($2\theta = 30.40^\circ$, 35.69° , 43.32° , 53.81° , 57.26° and 62.92°) [41].

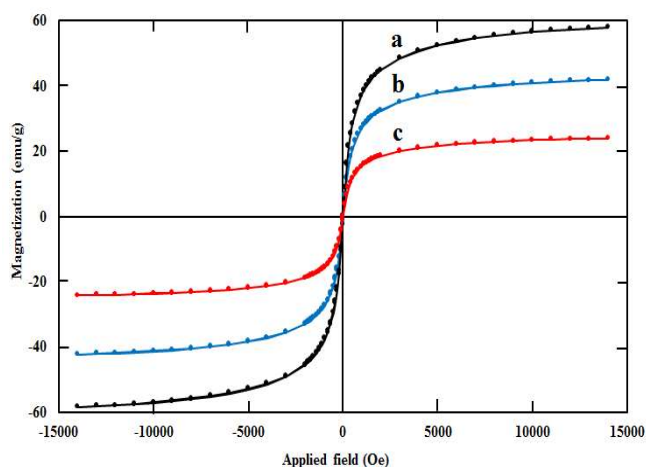


Fig. 5. The magnetization curves of (a) Fe_3O_4 , (b) $\text{Fe}_3\text{O}_4@SiO_2$ and (c) $\text{Fe}_3\text{O}_4@SiO_2@(CH_2)_3\text{-en-SO}_3\text{H}/H_2\text{SO}_4$.

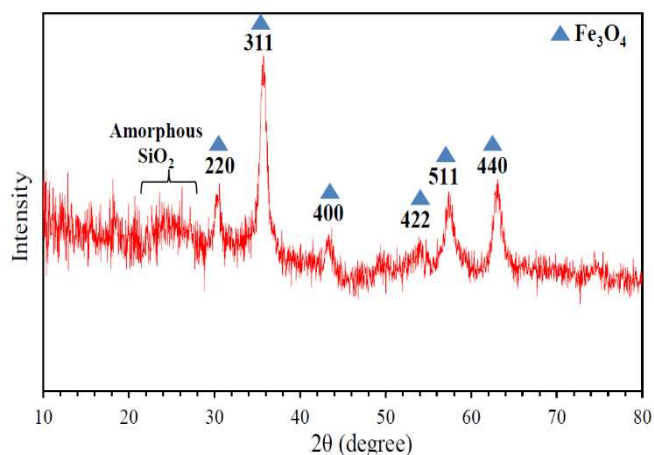


Fig. 6. XRD pattern of $\text{Fe}_3\text{O}_4@SiO_2@(CH_2)_3\text{-en-SO}_3\text{H}/H_2\text{SO}_4$.

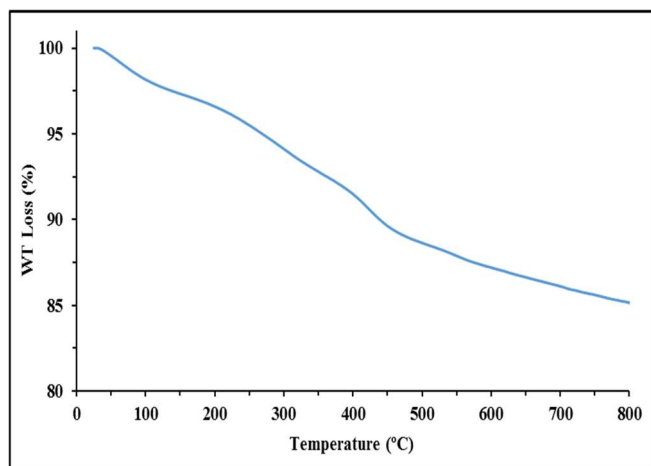


Fig. 7. TGA curve of $\text{Fe}_3\text{O}_4@\text{SiO}_2@(\text{CH}_2)_3\text{-en-SO}_3\text{H}/\text{H}_2\text{SO}_4$.

Figure 7 shows the thermal stability of the synthesized catalyst determined by thermogravimetric analysis (TGA) which displays two-step weight loss steps over the temperature range of TG analysis (25-800 °C). The first weight loss (~ 2.8%) below 150 °C might be ascribed to the removal of physically absorbed water and hydroxyl groups on the surface of the catalyst. The second weight loss (~ 12.1%) up to 200 °C can be ascribed to the breakdown and decomposition of organic moieties and thermal crystal phase

transformation [42].

Catalytic Activity

The catalytic efficiency of the prepared heterogeneous nanocatalysts was tested in the preparation of 2-aryl substituted benzoxazole. The reaction of benzaldehyde with 2-aminophenol was chosen as a model reaction to optimize the reaction conditions. After preliminary experiments, it was found that the best results were obtained when the reaction was carried out with 7 mol% of catalyst and solvent-free conditions (Table 1, entry 10). As shown in Table 1, the reaction was incomplete without the catalyst. The speed of the reaction increased with the increase of the amount of catalyst, and the reaction was completed by using 7 mol percent of the catalyst in the reaction. A higher amount of catalyst has no effect on the reaction rate or product yield. Also, by changing the reaction temperature, it can be seen that the reaction speed is directly proportional to the temperature and the best results were obtained at a temperature of 50 °C.

Also, the model reaction was studied in the presence of $\text{Fe}_3\text{O}_4@\text{SiO}_2@(\text{CH}_2)_3\text{-en-SO}_3\text{H}/\text{H}_2\text{SO}_4$ and its related intermediates (0.03 g) under solvent-free conditions at 50 °C for 30 min. The obtained data, as listed in Table 2, do not

Table 1. Optimization Study of the Reaction Conditions in the Condensation of Benzaldehyde with 2-Aminophenol

Entry	Catalyst (mol %)	Conditions	Time (min)	Yield (%)
1	10	H ₂ O, reflux	60	20
2	10	EtOH, reflux	60	30
3	10	EtOH:H ₂ O (1:1), reflux	60	30
4	10	EtOAc, reflux	60	40
5	10	MeCN, reflux	60	50
6	10	Neat, 80 °C	26	92
7	7	Neat, 80 °C	28	91
8	5	Neat, 80 °C	60	65
9	7	Neat, r.t.	60	40
10	7	Neat, 50 °C	30	91

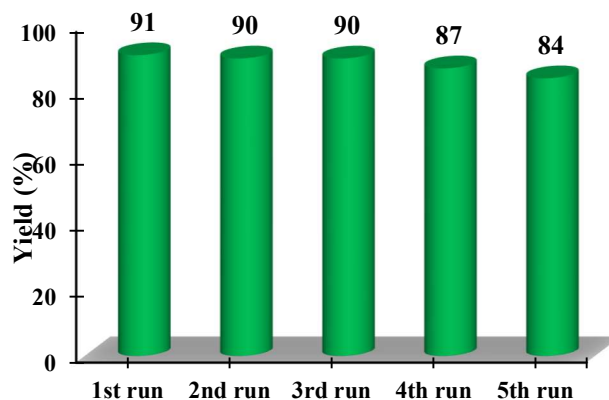
Table 2. Screening of the Model Reaction in the Presence of the Desired Catalyst and its Related Intermediates

Entry	Catalyst	Yield (%)
1	Fe ₃ O ₄	30
2	Fe ₃ O ₄ @SiO ₂	35
3	Fe ₃ O ₄ @SiO ₂ @(CH ₂) ₃ -Cl	35
4	Fe ₃ O ₄ @SiO ₂ @(CH ₂) ₃ -en	50
5	Fe ₃ O ₄ @SiO ₂ @(CH ₂) ₃ -en-SO ₃ H/HCl	80
6	Fe ₃ O ₄ @SiO ₂ @(CH ₂) ₃ -en-SO ₃ H/H ₂ SO ₄	91

show satisfactory results compared to Fe₃O₄@SiO₂@(CH₂)₃-en-SO₃H/H₂SO₄.

The optimal conditions for the conversion of aromatic aldehydes with electron-donating and electron-withdrawing groups to benzoxazole were investigated (Entry 1, Table 3). The results showed that all studied aryl aldehydes were completely converted to the corresponding 2-arylbzoxazoles with high efficiency and short reaction time. It is noteworthy that the reaction with aldehydes containing electron-donating groups such as 4-methylbenzaldehyde and 4-methoxybenzaldehyde took longer than the reaction with aldehydes containing withdrawing groups such as nitrobenzaldehydes. To determine the better efficiency of the catalyst, the number of circulation (TON) and frequency of circulation (TOF) are also calculated and shown in Table 3.

To determine the stability of the catalyst, it was magnetically separated from the reaction mixture after each run, washed with ethanol and ethane, then it was studied in the condensation reaction of benzaldehyde with 2-aminophenol in solvent-free conditions at a temperature of 50 degrees Celsius. It was dried in an oven at 60 degrees Celsius for one hour and used again. A small decrease in product yield (91%, 90%, 90%, 87%, and 84% in cycles 1-5, respectively) indicated that the catalyst could be recycled and

**Fig. 8.** Reusability of the catalyst.

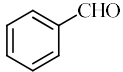
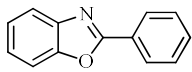
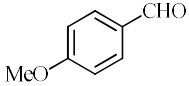
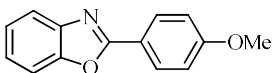
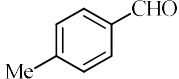
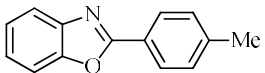
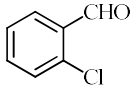
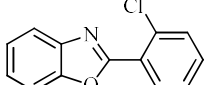
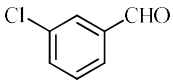
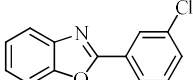
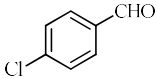
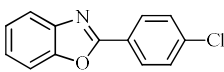
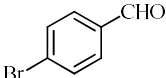
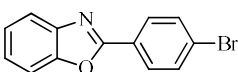
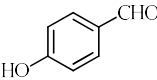
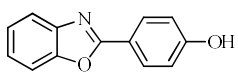
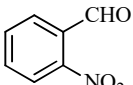
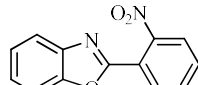
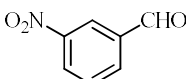
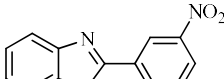
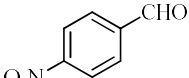
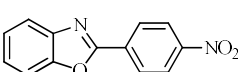
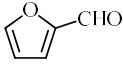
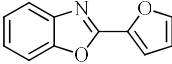
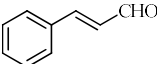
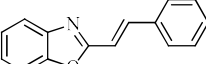
reused at least five times without a significant decrease in activity. Fig. 8).

The condensation reaction of 2-aminophenol and benzaldehyde was compared with Fe₃O₄@SiO₂@(CH₂)₃-en-SO₃H/H₂SO₄ catalyst and other catalysts. As shown in Table 4, the current method is better than the previous methods. Due to the high yield percentage, shorter reaction time, catalyst loading rate and environmental compatibility, it is dominant.

CONCLUSION

In conclusion, magnetic nanoparticles-supported sulfonated ethylenediamine was successfully synthesized and fully characterized by various techniques. The magnetic nanocomposite was then utilized in the synthesis of 2-arylbzoxazoles by the condensation reaction of various aromatic aldehydes with 2-aminophenol. The present method has many advantages over the previously reported procedures in terms of reduced reaction timings, higher yield, simplicity in operation and work-up, avoiding the application of dangerous acids or bases, environmentally friendliness, simple recovery of the nanomagnetic catalyst and reuse of the catalyst several times without a remarkable decrease in its activity.

Table 3. Synthesis of 2-Arylbenzoxazoles Catalyzed by Fe₃O₄@SiO₂@(CH₂)₃-en-SO₃H/H₂SO₄

Entry	Aldehyde	Product	Time (min)	Yield (%) ^a	m.p. (°C) [Ref.]	TON ^b	TOF (h ⁻¹) ^c
1			30	91	99-100 [8]	13.0	26.0
2			45	94	94-96 [8]	13.4	17.9
3			45	92	122-124 [8]	13.1	17.5
4			60	90	72-73 [6]	12.9	12.9
5			50	88	132-134 [6]	12.6	15.1
6			60	92	142-144 [8]	13.1	13.1
7			45	90	140-142 [8]	12.9	17.1
8			50	85	280-281 [8]	12.1	14.6
9			30	90	99-101 [6]	12.9	25.7
10			30	94	210-212 [6]	13.4	26.9
11			35	92	154-156 [12]	13.1	22.5
12			60	88	87-89 [6]	12.6	12.6
13			60	85	80-82 [8]	12.1	12.1

^aIsolated yields. ^bTON = mmol of product/mmol of catalyst. ^cTOF = TON/time of reaction.

Table 4. A comparative Analysis of the Effectiveness of Different Catalysts for the Preparation of 2-Phenylbenzoxazole

Entry	Catalyst (mol%)	Conditions	Time (h)	Yield (%)	Ref.
1	CuO-np/SiO ₂ (10)	MeOH, r.t.	7	80	[7]
2	Zn(OTf) ₃ (10)	EtOH, reflux	5	91	[10]
3	TiCl ₃ OTf (10)	EtOH, r.t.	2.2	80	[11]
4	BAIL gel (1)	Neat, 130 °C	5	98	[13]
5	PPC-SO ₃ H@MNP (8.7)	H ₂ O, reflux	0.75	87	[15]
6	Fe ₃ O ₄ @SiO ₂ @(CH ₂) ₃ -en-SO ₃ H/H ₂ SO ₄ (7)	Neat, 50 °C	0.5	91	This work

REFERENCES

- [1] V. Hessel, N.N. Tran, M.R. Asrami, Q.D. Tran, N.V.D. Long, M. Escribà-Gelonch, J.O. Tejada, S. Linke, K. Sundmacher, *Green Chem.* 24 (2022) 410.
- [2] V.J. Ram, A. Sethi, M. Nath, R. Pratap, Five-membered heterocycles, In *Chem. Heterocycles* 149 (2019).
- [3] R. Sattar, R. Mukhtar, M. Atif, M. Hasnain, A. Irfan, J. *Heterocycl. Chem.* 57 (2020) 2079.
- [4] F.Z. Foto, E. Foto, T. Ertan-Bolelli, I. Yildiz, *Bioorg. Chem.* 123 (2022) 105756.
- [5] A. Teimouri, A.N. Chermahini, H. Salavati, L. Ghorbanian, *J. Mol. Catal. A Chem.* 373 (2013) 38.
- [6] H. Sharma, N. Singh, D.O. Jang, *Green Chem.* 16 (2014) 4922.
- [7] S. Ramineni, R.K. Kannasani, V.V.S. Peruri, *Green Chem. Lett. Rev.* 7 (2014) 85.
- [8] J. Azizian, P. Torabi, J. Noei, *Tetrahedron Lett.* 57 (2016) 185.
- [9] A. Datta, *Orient. J. Chem.* 37 (2021) 341.
- [10] T.T. Nguyen, X.T.T. Nguyen, T.L.H. Nguyen, P.H. Tran, *ACS Omega* 4 (2019) 368.
- [11] K. Bahrami, M. Bakhtiarian, *ChemistrySelect* 3 (2018) 10875.
- [12] M. Sayyahi, M. Gorjizadeh, S. Sayyahi, *Iran. J. Catal.* 8 (2018) 203.
- [13] L.A. Nguyen, T.D. Dang, Q.A. Ngo, T.B. Nguyen, *Eur. J. Org. Chem.* 2020 (2020) 3818.
- [14] M. Beyki, M. Fallah-Mehrjardi, *Lett. Org. Chem.* 15 (2017) 39.
- [15] F. Najafi, M. Fallah-Mehrjardi, *Lett. Org. Chem.* 15 (2018) 778.
- [16] H. Talaei, M. Fallah-Mehrjardi, F. Hakimi, *J. Chin. Chem. Soc.* 65 (2018) 523.
- [17] R.S. Pottorf, N.K. Chadha, M. Katkevics, V. Ozola, E. Suna, H. Ghane, T. Regberg, M.R. Player, *Tetrahedron Lett.* 44 (2003) 175.
- [18] K.R. Kumar, P.V.V. Satyanarayana, B.S. Reddy, *J. Chem.* 2013 (2013) 151273.
- [19] Y.K. Liu, D. Mao, S. Lou, J. Qian, Z. Xu, *J. Zhejiang Univ. Sci. B.* 10 (2009) 472.
- [20] S.M. Inamdar, V.K. More, S.K. Mandal, *Tetrahedron Lett.* 54 (2013) 579.
- [21] O. Goli-Jolodar, F. Shirini, M. Seddighi, *Dye. Pigment.* 133 (2016) 292.
- [22] V.S. Shende, V.B. Saptal, B.M. Bhanage, *Chem. Rec.* 19 (2019) 2022.
- [23] H. Kargar, M. Fallah-Mehrjardi, R. Behjatmanesh-Ardakani, K.S. Munawar, M. Ashfaq, M.N. Tahir, *Transition Met. Chem.* 46 (2021) 437.
- [24] J.D. Tovar, F. Rataboul, L. Djakovitch, *Appl. Catal. A Gen.* 627 (2021) 118381.
- [25] Q. Peng, X. Zhao, M. Chen, J. Wang, K. Cui, X. Wei, Z. Hou, *Mol. Catal.* 517 (2022) 112049.

- [26] B. Karimi, S.J. Hoseini, K. Eskandari, A. Ghasemi, H. Nasrabadi, *Catal. Sci. Technol.* 2 (2012) 331.
- [27] B. Karimi, F. Mansouri, H.M. Mirzaei, *ChemCatChem* 7 (2015) 1736.
- [28] E.M. Materón, C.M. Miyazaki, O. Carr, N. Joshi, P.H. S. Picciani, C.J. Dalmaschio, F. Davis, F.M. Shimizu, *Appl. Surf. Sci. Adv.* 6 (2021) 100163.
- [29] X. Da, R. Li, X. Li, Y. Lu, F. Gu, Y. Liu, *Mater. Lett.* 309 (2022) 131357.
- [30] W. Ma, A.G. Ebadi, M.S. Sabil, R. Javahershenas, G. Jimenez, *RSC Adv.* 9 (2019) 12801.
- [31] M. Fallah-Mehrjardi, S. Sayyahi, *J. Sulfur Chem.* 42 (2021) 335.
- [32] M. Barzegar, A. Zare, A. Ghobadpoor, M. Dianat, *Iran. J. Catal.* 12 (2022) 13.
- [33] M. Fallah-Mehrjardi, S. Kalantari, *Org. Chem. Res.* 6 (2020) 137.
- [34] A.R. Kiasat, J. Davarpanah, *J. Mol. Catal. A. Chem.* 373 (2013) 46.
- [35] F. Xue, Y. Dong, P. Hu, Y. Deng, Y. Wei, *RSC Adv.* 5 (2015) 73684.
- [36] H. Alinezhad, M. Tajbakhsh, N. Ghobadi, *Synth. Commun.* 45 (2015) 1964.
- [37] J. Safari, Z. Zarnegar, *J. Mol. Catal. A. Chem.* 379 (2013) 269.
- [38] M. Fallah-Mehrjardi, S. Kalantari, *Russ. J. Org. Chem.* 56 (2020) 298.
- [39] M.Z. Kassaei, H. Masrouri, F. Movahedi, *Appl. Catal. A Gen.* 395 (2011) 28.
- [40] J. Safari, Z. Zarnegar, *J. Mol. Catal. A. Chem.* 379 (2013) 269.
- [41] M. Fallah-Mehrjardi, S. Kalantari, *Russ. J. Org. Chem.* 56 (2020) 298.
- [42] M.Z. Kassaei, H. Masrouri, F. Movahedi, *Appl. Catal. A Gen.* 395 (2011) 28.